PSFC/JA-19-40

Design of a Magnet and Gradient Coils for a Tabletop Liquid-Helium-Free, Persistent-Mode 1.5-T MgB_2 Osteoporosis MRI

Dongkeun Park, Yoonhyuck Choi, Yi Li, Wooseung Lee, Hiromi Tanaka,
Juan Bascuñán, Jerome L. Ackerman, Hideki Tanaka, Yukikazu Iwasa

April 2019

Plasma Science and Fusion Center
Massachusetts Institute of Technology
Cambridge MA 02139 USA

Thisworkwas supported by the National Institute of Biomedical Imaging and Bioengineering of theNational Institutes of Health underAward R01EB022062. Reproduction, translation, publication, use and disposal, in whole or in part, by or for the United States government is permitted.

Submitted to *IEEE Transactions on Applied Superconductivity*

Design of a Magnet and Gradient Coils for a Tabletop Liquid-Helium-Free, Persistent-Mode 1.5-T MgB_2 Osteoporosis MRI

Dongkeun Park, Yoonhyuck Choi, Yi Li, Wooseung Lee, Hiromi Tanaka, Juan Bascuñán, Jerome L. Ackerman, Hideki Tanaka, and Yukikazu Iwasa

***Abstract*—We have finalized the design of a full-scale tabletop 1.5-T/90-mm MgB_2 "finger" MRI magnet system for osteoporosis screening based on our preliminary test results of small coils and superconducting joints. The magnet will operate in persistent mode at 10 K with an additional 5 K temperature margin. The magnet design which includes six main coils and an iron shield satisfies the required specification of a field intensity of 1.5 T, homogeneity of $\leq$5 ppm over a 20-mm diameter of spherical volume, and a fringe field of $\leq$5 gauss at 0.5 m in radius from the magnet center. An active protection method using external heaters will be applied to prevent a local hot spot in the MgB_2 windings from being overheated when quench occurs. Active shield transverse and axial gradient coils for this tabletop osteoporosis MRI, having primary and shield coil pairs, are designed to minimize stray fields that can induce eddy currents on nearby metal surface and thus imaging artifacts. This paper covers design and analysis of: 1) the main coils and iron shield; 2) coil former; 3) quench protection; and 4) active shield gradient coils. We also discuss design changes of the cryostat and equipment plan for the overall system. The magnet system will be completed and then, equipped with other MRI hardware components including an in-house-made gradient coil assembly and RF coils for demonstration of 1.5-T finger MRI in 2020.**

***Index Terms*—Active shield gradient coil, Iron shielding, Magnesium diboride, MRI magnet, Tabletop MRI.**

I. Introduction

TABLETOP liquid-helium-free, persistent-mode 1.5-T/90-mm MgB_2 magnetic resonance imaging (MRI) magnet for osteoporosis screening has been developed at the Francis Bitter Magnet Laboratory (FBML)/Plasma Science and Fusion Center (PSFC), MIT since 2017. We set the design requirement specification for this tabletop MRI magnet and determined to use a passive shielding method, using an iron yoke, to meet one of the key requirements, a 5-gauss line radius of $\leq$0.5 m [1]. One remarkable feature is to use a solid nitrogen cooling in temperature range of 10—15 K, enabling, by its thermal mass, the magnet to operate several hours with cryocooler turned off, thus, allowing imaging under a quiescent environment. We have successfully developed a technique to make a superconducting joint carrying >200 A at 15 K in self-field with unreacted, monofilament MgB_2 wires [2]–[4]. We built and tested two solid-nitrogen-cooled, persistent-mode 1.8-T/20-mm-cold-bore test coils, each wound-and-reacted with a ~90-m long mono-filament MgB_2 wire made by Hitachi Research Laboratory, and successfully demonstrated the pesistent-mode operation of 0.17 ppm/hr, corresponding to a joint resistance of $1.45\times10^{-13}\Omega$, at 16 K [5], [6]. From these test coil experiments, we have validated actual winding dimension, heat-treatment, solid nitrogen cooling, wire performance in field, persistent switch operation, and superconducting joint results, all the essentials for an MgB_2 MRI magnet. In the following Section II, we present a design method and results of main coils and an iron shield for a full-scale magnet. We also compute the temperature rise in the case of local quench and propose a protection method. In Section III, we describe a gradient coil design method and 1^{st}-cut results. A new cryostat design, modified from the previously proposed one [1], and an overall system composition are described in Section IV. A full-scale tabletop 1.5-T/90-mm MgB_2 MRI magnet will be manufactured and demonstrated in 2020.

Research reported in this publication was supported by the National Institute of General Medical Sciences of the National Institutes of Health under award number R01EB022062. (Corresponding author: Dongkeun Park)

D. Park, Y. Choi, Y. Li, W. Lee, H. Tanaka, J. Bascuñán and Y. Iwasa are with the Francis Bitter Magnet Laboratory/Plasma Science and Fusion Center, Massachusetts Institute of Technology, Cambridge, MA 02139, USA (e-mail: dk_park@mit.edu).

J. L. Ackerman is with the Martinos Center for Biomedical Imaging, Department of Radiology, Massachusetts General Hospital, Charlestown, MA 02129, USA (e-mail: jerry@nmr.mgh.harvard.edu)

H. Tanaka is the Research and Development Group, Center for Technology Innovation—Energy, Hitachi Ltd., Hitachi-shi 3191221, Japan (e-mail: hideki.tanaka.cj@hitachi.com)

II. Design of a Tabletop Iron-shielded 1.5-T MgB_2 MRI Magnet

A. MgB_2 Wire Specification and Performance

We selected the same wire used in [6], a ϕ0.64-mm bare/ϕ0.78-mm T-glass-insulated, unreacted, mono-filament MgB_2 wire made by Hitachi. The unreacted MgB_2 core contains undoped *in situ* powder mixture of a magnesium (>99.5%, –325 mesh) and an amorphous nano boron (98.90%, <250 nm) supplied by Pavezyum, Turkey. Fig. 1 shows the I_c data of the short samples extracted from both ends of the 1.4-km MgB_2 wire to be used for our full-scale tabletop MRI magnet. Samples were sintered at 600°C for 12 hours in an argon gas atmosphere. The wire is composed of a single-core MgB_2 with 34% fraction and outside layers of an iron sheath and a copper stabilizer of which filling rates are 32% and 34%, respectively. The $I_c(B,T)$ and equivalent electrical and thermal properties were used for the magnet design and quench analysis described in following subsections.

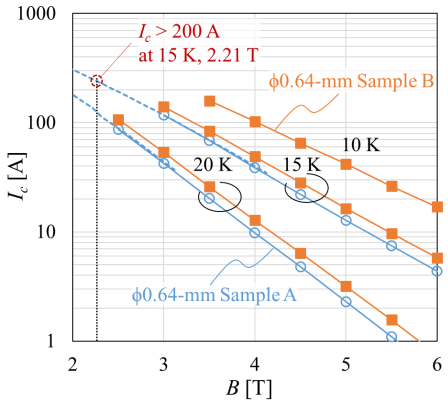

Fig. 1. Ic-B data provided from Hitachi. Samples A and B are extracted from both ends of the 1.4 km wire delivered to MIT. Dashed lines are fitting curve with Jc-B of previous wire measured by magnetization method [7].

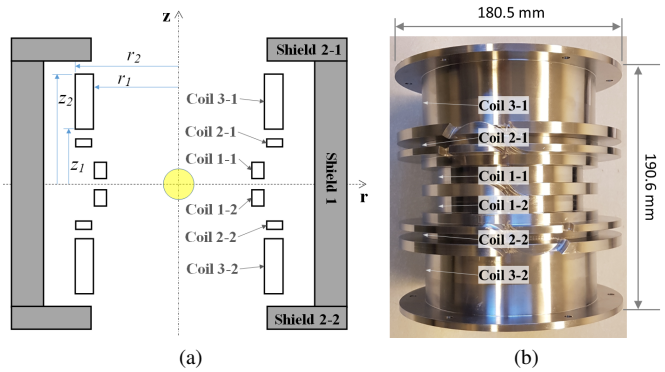

Fig. 2. Configuration of an optimized tabletop MRI magnet: (a) To-scale cross-section profile of main coils and an iron shield; and (b) a photo of the manufactured former (arrows indicate winding direction).

B. Optimization of MgB_2 Main Coils with an Iron Shield

The positions and boundaries of the superconducting coil windings are constrained by design required specifications [1] and optimized with the Hitachi MgB_2 wire and the iron shield. We have increased a design target homogeneous volume to 25 mm in diameter spherical volume (DSV) while maintaining similar amount of wire length thanks to enhanced MgB_2 wire in-field performance. We expect to reduce high-order harmonic errors in the required imaging volume of 20-mm DSV and thus significantly reduce a burden of shimming. An optimization for the main coil has been done by using first a linear program and then a non-linear Genetic Algorithm with Simulated Annealing [8], [9]. Cost function is evaluated with different penalty weightings of parameters within the confined coil boundaries based on achieving the center field of 1.35 T and reducing inhomogeneity. Here, we put zero weighting for a fringe field parameter. We use an operating current, I_{op}=105 A, less than 55% of the critical current, I_c, at the peak field in coils to operate reliably in persistent mode at $\geq$15 K. Coil positions are modified with a surrounding iron-shield taken into account by using 2D finite element method (FEM) to achieve the center field of 1.5 T, the 5-gauss fringe field radius of $\leq$0.5 m, and inhomogeneity in 25-mm DSV of $\leq$5 ppm. Finally, we refine the design by using a 3D FEM model with detailed figuration of the iron shield including its alignment holes.

Table I shows optimized design parameters of the iron-shielded 1.5-T MRI magnet. Fig. 2(a) shows a to-scale cross-section profile of the designed magnet. The equivalent wire dimension of 0.86$\times$0.73 mm^2, determined by our preliminary winding experiences with the same wire and tension, is used for design optimization because the actual dimension of a ϕ0.78-mm T-glass insulated wire is deformed during winding. From the optimization result, we obtained the final coil positions to meet the target homogeneity. Since both temperature and force change the dimension of each coil, impacting field homogeneity, the RT dimensions in manufacturing must include dimensional changes that each coil is subjected to when the coils are cooled and energized. Fig. 2(b) shows a photo of the former, made of Stainless Steel 304 which has Youngś modulus of 200 GPa and thermal contraction from RT to 10 K of 0.296%. We computed the RT dimensions of the former considering thermal contraction during cool-down and deformation by electromagnetic force during energization.

Our tabletop MgB_2 MRI magnet will be operated in persistent mode. Main coils and a non-inductive persistent switch will be wound with a continuous wire and two ends of the wire will be joined by a superconducting joint. The peak field in Coil 3-1 (and its symmetric counterpart Coil 3-2) is 2.21 T and the percentage ratio, I_{op}/I_c is $\sim$45% at 2.21 T, 15 K as shown in Fig. 1. To achieve a required temporal stability of $<$0.1 ppm/hr considering the inductance of 720 mH and a non-zero resistance of the MgB_2 coil due to index number, n $>$40 (at 2.21 T and 15 K), a joint resistance must be $<2\times10^{-11}\Omega$, readily achievable. Computed inhomogeneity of 6.4 ppm in 25-mm DSV is slightly above the target 5 ppm as shown in Fig. 3(a), but still meets the required 5 ppm in 20-mm DSV. Inhomogeneity of the as-manufactured magnet will fail to meet the specification due chiefly to dimensional tolerances of coil forms and wires. The average probable field error caused by combinations of axial/radial movements of each coil block by 1 mm, i.e. the field error sensitivity, is computed and listed in Table I. The former was manufactured with the maximum dimensional tolerance of 10 μm. This indicates that a geometry-induced error field may be limited to $<$140 ppm and then, inhomogeneity can be reduced to $<$5 ppm, the target MRI-quality field, by a ferromagnetic shim method. Fig. 3(b) shows a plot of the 5-gauss fringe field line which meets the required specification of $\leq$0.5 m.

The wind-and-react method will be used for our MgB_2 coil, so the former will be heat-treated together with the unreacted MgB_2 wire on it. We ignore a possible small irreversible deformation during heat treatment. After heat-treatment we consider to do a wax-impregnation on the coil windings to prevent the wire movement. The maximum hoop stress, σ_ϕ of 26 MPa in the coil winding is manageable. We will place a superconducting joint in $<$0.25 T region, between 0.25-T line and Shield 1 near mid-plane. The iron shield is made of a stack of 0.5-mm thick silicon steel NGO 50PN1300 sheets. Two types of sheets, Shield 1 and 2 are designed and cut by a laser cutter.

TABLE I
DESIGN PARAMETERS OF THE IRON-SHIELDED 1.5-T MgB_2 MAGNET FOR THE TABLETOP *Finger* MRI

Parameters	**Coil 1-1***	**Coil 2-1***	**Coil 3-1***
Equiv. wire dimension	0.86 mm × 0.73 mm		
$2r_1$; $2r_2$ [mm]	120.00; 138.98	144.00; 168.82	140.00; 169.20
z_1; z_2 [mm]	4.62; 17.52	30.46; 37.34	45.28; 90.00
# turns/layer; # layers	15; 13	8; 17	52; 20
Total wire length [m]	1,303 (for all 6 coils)		
I_{op} [A]	105		
Center field [T]	1.5		
Max. field in coil [T]	1.73	1.45	2.21
Max. σ_ϕ [MPa]	17.4	17	26
Total inductance [mH]	720 (stored energy: 3.97 kJ)		
Homogeneity [ppm]	6.4 (peak-to-peak) in 25-mm DSV		
Field sensitivity [ppm/mm]	5650	1820	6270
5-gauss line [m]	(Radial) 0.48; (Axial) 0.69		
T_{op} [K]	10 — 15		
Iron Sheld	**Shield 1**	**Shield 2-1***	
Material	0.5-mm thick Silicon Steel NGO 50PN1300		
$2r_1$; $2r_2$ [mm]	220.00; 270.00	144.00; 270.00	
z_1; z_2 [mm]	-100.80; 100.80	100.80; 119.76	
# stack	404	2 × 38	

* mid-plane symmetry.

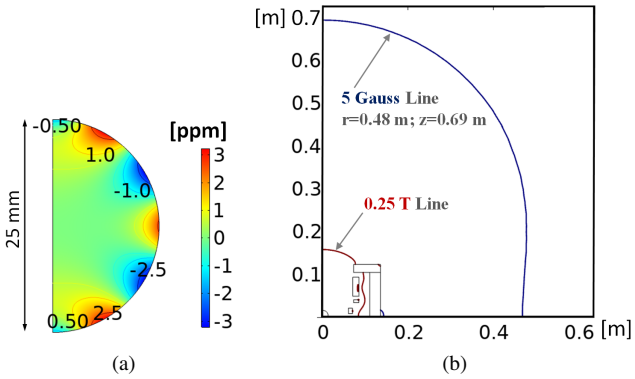

Fig. 3. Computation results: (a) Homogeneity in ppm in ROI; and (b) 5-gauss and 0.25-T field line.

C. Quench Analysis and Active Protection Method

We computed the quench propagation in Coil 3-1, which has relatively small margin and high internal stress, with a semi-analytical method to solve multiple differential equations [10], [11]. Fig. 4 shows quench analysis results of Coil 3-1: (a) the peak temperature vs. time; and (b) the spatial temperature distribution. If we assume that a local hot spot occurs and quenches at 10 K at the one full innermost turn in Coil 3-1, the peak temperature increases up to 300 K in 4 seconds. Coil 3-1 is conservatively assumed to be under adiabatic condition, i.e., thermal isolation. A computed initial normal zone propagation velocity (NZPV) in Coil 3-1 is ∼0.5 m·s^{-1} at T_{op}=10 K and the current sharing temperature, T_{cs}, is 25 K. Unlike low-temperature superconductor (LTS)-based MRI magnets that rely on passive protection, MgB_2 magnet must rely on active protection because of its relatively slow NZPV. Although

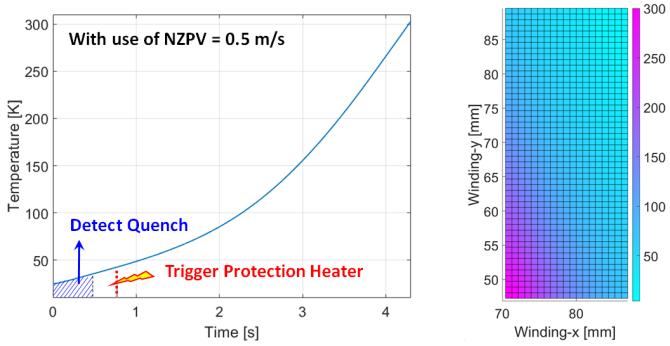

Fig. 4. Quench analysis results of Coil 3-1 at I_{op}=10 K : (a) peak temperature vs. time; and (b) spatial temperature distribution.

MgB_2 magnets are not susceptible to quench by disturbances that still afflict LTS magnets due to >100 times higher stability margin of MgB_2 (energy density margin, Δe_h=0.35 J·cm^{-3}) than that of NbTi ($\Delta e_h < 3 \times 10^{-3}$ J·cm^{-3}) [11], for this tabletop 1.5-T MgB_2 magnet we apply the active protection technique by using a quench protection heater and a capacitor-type firing circuit demonstrated with a test coil [12] and used successfully in our 0.5-T/240-mm cold bore magnet [13].

In case of a magnet quench initiated in any coil, quench heaters attached on outer surfaces of Coil 3-1 and Coil 3-2 are activated by an external heater-current-firing circuit, forcing both largest coils to be quenched from the outer layers and thus absorb the magnet stored energy. If we assume two layers from both coils, the most conservative assumption, a total winding length of 110 m (35.2 cm^3, 8.5% of a whole coil volume), absorb 3970 J, its enthalpy density will be increased to 105 J·cm^{-3}, which translates to a final temperature of below 155 K, a safe level. For example, if a quench is detected in 0.5 second after quench occurs, we can dump the heater energy of 10 J to increase temperature of 110 m wire from 10 K to 40 K for 0.3 second, i.e. ∼33 W heater required. We will optimize a quench and protection code for this tabletop 1.5-T MgB_2 magnet before heater installation and operation.

III. DESIGN OF GRADIENT COILS FOR A FINGER MRI

To design active shield gradient coils for the tabletop 1.5-T/90-mm MRI magnet, we developed a code to compute the magnetic field distribution arising from an arbitrary wire path in 3D space based on the Biot-Savart formula. Wire paths in 3D space are defined with a series of commands specifying straight segments and arcs for a Z gradient, "fingerprint" spirals on a cylinder for X and Y gradients. The Biot-Savart formula can be evaluated in an octant of space for unit current in the full wire path because of the inherent symmetries of the gradient coils. Inductance is computed by summing the squared magnitude of the field. Dynamic effects such as eddy current generation in nearby metallic structures are not taken into account. The conformance to the target field is evaluated: desired gradient within a 25-mm DSV; and zero field outside the gradient to minimize eddy currents. The parameters defining the wire path, e.g. the

TABLE II
1ST-CUT DESIGN RESULTS OF AN ACTIVE SHIELD GRADIENT COIL SET FOR A TABLETOP *Finger* MRI

Parameters	Transverse X, Y	Axial Z
Gradient strength [mT/m/A]	13.20	8.22
Tube radius of primary; shield [mm]	21; 34	27; 40
Wire length [m]	7.25	5.4
Minimum turn spacing [mm]	0.90	1.19
Resistance* [Ω]	1.08	0.80
Inductance [μH]	0.98	0.31

*Linear resistivity of 0.14-mm thick × 0.812-mm wide, 149 mΩ/m

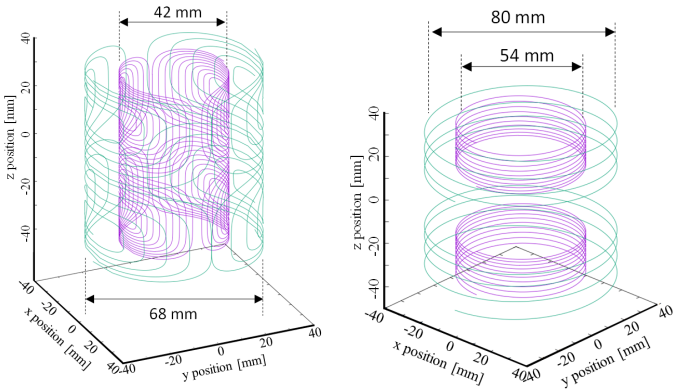

(a) (b)

Fig. 5. Wire paths of active shield gradient coils: (a) Transverse gradient, X or Y ; and (b) axial gradient, Z.

coefficients of a polynomial describing the axial wire spacing of the z-gradient, are optimized with a Levenberg-Marquardt nonlinear least squares algorithm giving chosen weighting to conformity with the target fields, power dissipation and self-inductance. The first-cut design results are listed in Table II and Fig. 5 shows wire paths of a transverse, X or Y, gradient in (a) and an axial Z gradient in (b). With powering each gradient coil by the gradient amplifier (Techron 2015) up to 16 A, the maximum transverse and axial gradient strengths will be 211 mT·m^{-1} and 131 mT·m^{-1}, respectively, sufficient to achieve 50 μm in plane resolution. The maximum power dissipations in the transverse and axial gradient coils will be 276 W and 205 W, respectively. In this gradient assembly, we will insert ϕ6.35 mm tubes for water cooling and 5-mm thick pockets for ferromagnetic shimming in a 7-mm annular space between primary coils and shield coils.

IV. CRYOSTAT AND OVERALL SYSTEM

Fig. 6 shows a schematic view of an overall system. We have changed a cryostat design to make its construction and assembly simpler and more convenient compared with the previous design [1]: (1) new single size RT bore of 90 mm, still possible to insert a hand vs. previous 2-step RT bore of 102 mm and 90 mm; and (2) new open-ended bore for routing wires, power cables and cooling tubes from a gradient assembly vs. previous one-end-closed bore. The mounting position of a cryocooler should be off center that makes outer

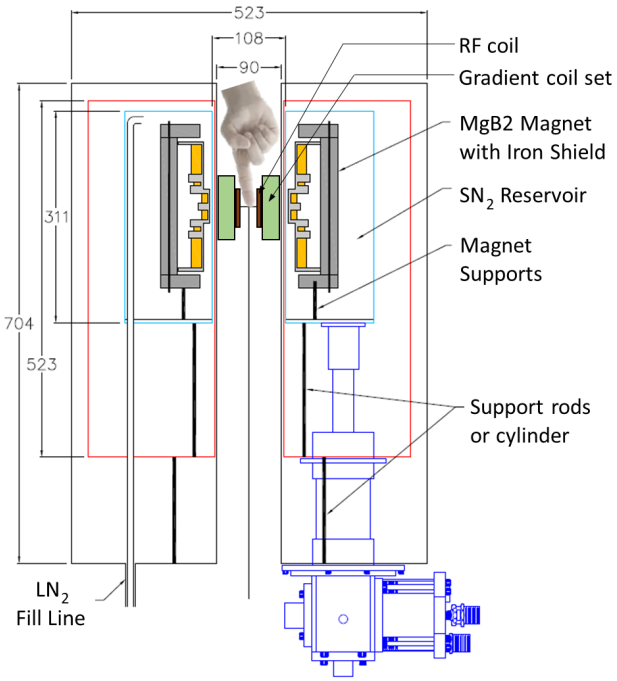

Fig. 6. Overall system view of the tabletop MgB2 "finger" MRI

diameter of a new cryostat (524 mm) larger than the previous cryostat design (378 mm). A volume of solid nitrogen will be ∼20 liter in the cold chamber and we estimate that a cooling time from 77 K (liquid) to 10 K (solid) can be ∼30 hours by a RDK-408S (6 W at 10 K) cryocooler. If an average heat input to the cold-chamber is 2.5 W when the cryocooler is off, the magnet can remain in the operating temperature range, from 10 to 15 K, for ∼4 hours. An accurate cryostat heat input including a heat generation by magnet-gradient coil interactions will be further investigated. We plan to turn off the cryocooler intentionally to provide a quiescent—noise-free—environment during imaging. A redesigned cryostat is now under construction. A gradient coil assembly with an outside diamter of 80 mm and an inside diameter of 42 mm will readily fit into the magnet bore and have sufficient inside bore space for 2.5-mm thick in-house made RF coils. A Tecmag Bluestone imaging console, gradient amplifiers, RF power amplifiers and other imaging components will be equipped at the MIT FBML/PSFC in 2020 for demonstration of our tabletop 1.5-T MgB_2 osteoporosis MRI magnet.

V. CONCLUSION

The final design results of the iron-shielded 1.5-T/90-mm MgB_2 osteoporosis MRI magnet and the first-cut design results of the active shield gradient coils are reported. The optimized magnet assembly requires a total ∼1.3 km of MgB_2 wire and ∼43 kg of silicon steel. We will apply an active protection method for reliable operation, although MgB_2 is immune to quench. The first-cut design result of shielded gradient assembly with gradient strengths of 13.2 (transverse) and 8.2 mT·m^{-1}·A^{-1} (axial) are reported and discussed. We will complete this tabletop solid-nitrogen-cooled persistent 1.5-T MgB_2 magnet construction and operation in 2020.

REFERENCES

[1] D. Park, J. Bascuñán, P. C. Michael and Y. Iwasa, "A Tabletop Persistent-Mode, Liquid-Helium-Free, 1.5-T/90-mm MgB2 "Finger" MRI Magnet for Osteoporosis Screening: Two Design Options," *IEEE Trans. Appl. Supercond.*, vol. 28, no. 3, 4400105, 2018.

[2] W. Yao, J. Bascuñán, S. Hahn, and Y. Iwasa, "A superconducting joint technique for round wires," *IEEE Trans. Appl. Supercond.*, vol. 19, no. 3, pp. 2261–2264, 2009.

[3] D. K. Park, J. Ling, M. Rindfleisch, J. Voccio, S. Hahn, J. Bascuñán, M. Tomsic, and Y. Iwasa, "MgB2 for MRI magnets: Test coils and superconducting joints results," *IEEE Trans. Appl. Supercond.*, vol. 22, no. 3, pp. 3–7, 2012.

[4] J. Ling, J. Voccio, Y. Kim, S. Hahn, J. Bascuñán, D. K. Park, and Y. Iwasa, "Monofilament MgB2 wire for a whole-body MRI magnet: Superconducting joints and test coils," *IEEE Trans. Appl. Supercond.*, vol. 23, no. 3, pp. 10–13, 2013.

[5] Y. H. Choi, Y. Li, D. Park, J. Lee, P. C. Michael, J. Bascuñán, J. P. Voccio, Y. Iwasa and H. Tanaka, "A Tabletop Persistent-Mode, Liquid Helium-Free 1.5-T MgB2 "Finger" MRI Magnet: Construction and Operation of a Prototype Magnet," *IEEE Trans. Appl. Supercond.*, vol. 29, no. 5, 4400405, 2019.

[6] Yoonhyuck Choi, Yi Li, Dongkeun Park, Wooseung Lee, Hiromi Tanaka, Juan Bascuñán, Yukikazu Iwasa, and Hideki Tanaka, "A Tabletop, Liquid Helium-Free, Persistent-Mode 1.5-T MgB2 "Finger" MRI Magnet: Small-Scale Test Coil Results and Final Design Review," presented at the 26th Internation Conference on Magnet Technology, Tue-Mo-Or9.05, Sep. 24, 2019.

[7] M. Kodama, T. Suzuki, H. Tanaka, K. Okishiro, K. Okamoto, Gen Nishijima, A. Matsumoto, A. Yamamoto, J. Shimoyama, K. Kishio, "High-performance dense MgB_2 superconducting wire fabricated from mechanically milled powder," *Supercond. Sci. Technol.*, 30, 4, 044006, 2017.

[8] N. R. Shaw, and R. E. Ansorge, "Genetic algorithms for MRI magnet design," *IEEE Trans. Appl. Supercond.*, vol. 12, no. 1, pp. 733–736, 2002.

[9] H. Xu, S. M. Conolly, G. C. Scott, and A. Macovski, "Homogeneous magnet design using linear programming," *IEEE Trans. Magnetics*, vol. 36, no. 2, 476-483, 2000.

[10] Wooseung Lee, Dongkeun Park, Yukikazu Iwasa, Junseong Kim, Jiho Lee, and Do Gyun Kim, "Quench Analysis of an LTS Quadrupole Triplet Magnet System for the IBS RAON Inflight-Fragment Separator," presented at the 26th Internation Conference on Magnet Technology, Wed-Mo-Po3.11-02, Sep. 25, 2019.

[11] Yukikazu Iwasa, Case Studies in Superconducting Magnet, 2nd Edition, Springer, 2009.

[12] D. K. Park, S. Hahn, J. Bascuñán, and Y. Iwasa, "Active protection of an MgB2 test coil," *IEEE Trans. Appl. Supercond.*, vol. 21, 2402, 2011.

[13] J. Ling, J. P. Voccio, S. Hahn, T. Qu, J. Bascuñán, and Y. Iwasa, "A persistent-mode 0.5T solid-nitrogen-cooled MgB2 magnet for MRI," *Supercond. Sci. Technol.*, vol. 30, 024011, 2017.